CONFIDENTIAL
DECLASSIFIED

Copy 307
RM L51B15

NACA RM L51B15

NACA

RESEARCH MEMORANDUM

FREE-FLIGHT INVESTIGATION OF THE LONGITUDINAL STABILITY AND CONTROL OF A ROCKET-PROPELLED MISSILE MODEL HAVING CRUCIFORM, TRIANGULAR, INTERDIGITATED WINGS AND TAILS

By Carl A. Sandahl and James R. Hall

Langley Aeronautical Laboratory
Langley Field, Va.

Declassified by authority of NASA
Classification Change Notices No. 143
Dated ** 2-14-8

CLASSIFIED DOCUMENT

This document contains classified information affecting the National Defense of the United States within the meaning of the Espionage Act, USC 50:31 and 32. Its transmission or the revelation of its contents in any manner to an unauthorized person is prohibited by law.
Information so classified may be imparted only to persons in the military and naval services of the United States, appropriate civilian officers and employees of the Federal Government who have a legitimate interest therein, and to United States citizens of known loyalty and discretion who of necessity must be informed thereof.

NATIONAL ADVISORY COMMITTEE FOR AERONAUTICS

WASHINGTON
July 10, 1951

CONFIDENTIAL

DECLASSIFIED
~~CONFIDENTIAL~~

NATIONAL ADVISORY COMMITTEE FOR AERONAUTICS

RESEARCH MEMORANDUM

FREE-FLIGHT INVESTIGATION OF THE LONGITUDINAL STABILITY AND CONTROL OF A ROCKET-PROPELLED MISSILE MODEL HAVING CRUCIFORM, TRIANGULAR, INTERDIGITATED WINGS AND TAILS

By Carl A. Sandahl and James R. Hall

SUMMARY

The Pilotless Aircraft Research Division of the Langley Aeronautical Laboratory has flight-tested a missile model having cruciform, triangular, interdigitated wings and tails to determine longitudinal stability and control characteristics over the Mach number range from 0.75 to 1.5. The results obtained with the center of gravity located at 50.8 percent of the mean aerodynamic chord of the exposed wing area are presented herein. The normal-force slopes were relatively uniform over the Mach number range. Static stability existed over the Mach number range and was a maximum at a Mach number of 0.95. Damping was maintained but the total damping-moment coefficient was considerably lower at supersonic than at subsonic speeds. Control effectiveness was maintained and was lower at supersonic speeds than at subsonic speeds probably because of the absence of the effects of downwash changes in the vicinity of the tail for the small wing deflections employed. The hinge moments of the control wing were reasonably well-balanced at supersonic speeds, but overbalanced at subsonic speeds.

INTRODUCTION

The Pilotless Aircraft Research Division of the Langley Aeronautical Laboratory is investigating some of the aerodynamic characteristics of

a missile having cruciform, triangular, interdigitated wings and tails. One phase of the program - the measurement of the variation of zero-lift drag with Mach number for several configurations similar to the one of the present tests - has been completed and the results reported (reference 1). Tests are currently underway to determine the longitudinal stability and control characteristics of several configurations. The first results, obtained with a model having the interdigitated-tail arrangement, are presented herein. The flight test was conducted at the Pilotless Aircraft Research Station, Wallops Island, Va.

SYMBOLS

C_N	normal-force coefficient $\left(\frac{\text{Normal force}}{qS}\right)$
C_m	pitching-moment coefficient $\left(\frac{\text{Pitching moment}}{qS\bar{c}}\right)$
C_h	wing hinge-moment coefficient $\left(\frac{\text{Hinge moment}}{qS\bar{c}}\right)$
q	dynamic pressure, pounds per square foot
S	exposed area of two wing panels, 3.21 square feet
$\bar{c}$	mean aerodynamic chord of exposed wing, 1.572 feet
c_r	wing chord at wing-fuselage juncture
α	angle of attack, degrees
θ	angle of pitch, degrees
δ	wing deflection angle, positive when leading edge is up, degrees
M	Mach number
P	period of longitudinal oscillation, seconds
$T_{1/2}$	time to damp oscillations to one-half amplitude, seconds
a.c.	aerodynamic center
V	flight velocity, feet per second
t	time, seconds

Subscripts:

$\dot{\alpha} = \frac{d\alpha}{dt}\frac{\bar{c}}{2V}$

$q = \frac{d\theta}{dt}\frac{\bar{c}}{2V}$

T trim

Subscripts used with coefficients indicate partial derivatives, that is, $C_{N_\alpha} = \frac{\partial C_N}{\partial \alpha}$.

All angles and angular velocities are in degrees and degrees per second.

MODEL AND TEST PROCEDURES

The general arrangement of the model is shown in figures 1 and 2 and additional information is given in table I.

The fuselage was constructed of 0.064-inch-thick 75S-T aluminum with ring stiffeners except at the wing and tail sections which were forged and machined. The wings and tails were forged and machined from 24S-T aluminum.

The vertical wings and the four tail surfaces were fixed at zero incidence. A pneumatic pulsing system moved the horizontal wings in a square-wave motion. The wing deflection angles varied from $\pm 1.8^\circ$ at $M = 0.75$ to $\pm 1.5^\circ$ at $M = 1.5$. The dwell time was 1 second. The magnitudes of the wing deflection angles were limited by structural limitations of the model.

The model was propelled to a Mach number of about 1.0 by a rocket booster which produced an impulse of 19,800 pound-seconds (average thrust equaled 6500 lb). After the boost period the model was accelerated to a Mach number of 1.6 by a special 65-inch rocket sustaining motor which produced an impulse of 7700 pound-seconds (average thrust equaled 7300 lb). A photograph of a model and booster on the launcher is shown in figure 3.

A standard NACA telemeter was installed in the nose section. The quantities measured included normal, lateral, and longitudinal accelerations, angle of attack, total pressure, wing deflection angle, and wing hinge moment. The model was tracked with SCR 584 and Doppler radars to obtain space coordinates and flight-path velocity, respectively. The flight-path velocity was also obtained from telemetered values of total pressure. Ambient atmospheric conditions were obtained by means of radiosonde equipment. The Reynolds number, based on the wing mean aerodynamic chord (1.572 ft), varied from 5,850,000 at $M = 0.75$ to 14,000,000 at $M = 1.5$.

RESULTS AND DISCUSSION

The results presented herein were obtained during power-off coasting flight from measurements made during the short-period longitudinal oscillations produced by the abrupt changes in wing deflection and during trim conditions following damping of the oscillation. The longitudinal static stability and damping derivatives were obtained from the period and damping of the short-period longitudinal oscillation. A typical portion of the time history showing an oscillation is given in figure 4. The derivatives C_{N_α} and C_{h_α} were evaluated from measurements of normal acceleration, wing hinge moment, and angle of attack during the short-period oscillation while the wing incidence was fixed. The derivatives C_{N_δ} and C_{h_δ} were calculated from the increments in successive trim values of the normal acceleration and wing hinge moment, taking into account the effect of the change in trim angle of attack. The quantity C_{m_δ} was obtained by using values of C_{m_α} and trim values of α/δ obtained from direct measurements. A more complete description of the method is given in reference 2.

Normal-force slope.- The variation of C_{N_α} with Mach number is shown in figure 5. The scatter evident at low supersonic speeds may be due in part to the small angle-of-attack ranges (approx. 1°) available for the determination of C_{N_α} in this speed range. The slopes of the normal-force curves were relatively uniform over the Mach number range investigated and at the highest Mach numbers were about 12 percent lower than the subsonic values. Satisfactory agreement was obtained with subsonic and supersonic wind-tunnel tests of a similar configuration, references 3 and 4, respectively.

Static stability and damping.- The variation of the period and the time to damp to one-half amplitude of the longitudinal oscillations measured during the flight test are shown in figure 6; values of C_{m_α}

obtained from these quantities are shown in figure 7. The results indicate static stability over the Mach number range investigated with a substantial increase at transonic speeds and a peak at $M = 0.95$. Also shown in figure 7 are values of C_{m_α} for $\alpha = \delta = 0$ obtained in wind-tunnel tests of a similar configuration (references 3 and 4) and transferred to the center-of-gravity location of the present test. The present flight-test results indicate less static stability than do the wind-tunnel tests. Unpublished calculations indicate that the differences are due mainly to the aeroelastic behavior of the tails, the effects of which are considerably larger for the flight models (constructed of duralumin) than for the wind-tunnel model (constructed of steel). The dynamic pressure in the flight tests is also much higher than that in the wind-tunnel tests.

The variation of aerodynamic center with Mach number obtained in the present test is shown in figure 8 and compared with aerodynamic-center locations calculated from values of C_{m_α} obtained at the U.S. Naval Air Missile Test Center at Pt. Mugu, Calif., for a similar configuration and values of C_{N_α} from the present tests. Also shown are wind-tunnel results for a similar configuration from references 3 and 4. The flight results indicate a more forward location of aerodynamic center. The difference in aerodynamic-center location is about 8 percent of the wing mean aerodynamic chord at $M = 1.5$ and represents a difference of 1 percent of the fuselage length.

The total damping factor $C_{m_q} + C_{m_{\dot{\alpha}}}$ is shown in figure 9. Damping was maintained over the Mach number range investigated; the total damping-moment coefficient was considerably lower at supersonic than at subsonic speeds.

Control effectiveness.- The variations of C_{N_δ} and $C_{N_{\delta_T}}$, the increment in trim normal-force coefficient due to unit control wing-deflection angle, shown in figure 10 indicate that the normal force due to control wing deflection was maintained over the Mach number range. The ratio of C_{N_δ} to C_{N_α} varied from about 0.5 at $M = 0.75$ to 0.7 at $M = 1.5$. The present values of C_{N_δ} are higher than the wind-tunnel values for a similar configuration (references 3 and 5) shown in figure 10. The wind-tunnel results indicate lower values of C_{N_δ} with the tail on than with the tail off because of the wing downwash at the tail location. The present results generally agree more closely with the tail-off tunnel results than with the tail-on results; this agreement indicates that in the present tests the changes in downwash

at the tail location were either negligible or did not occur in the vicinity of the interdigitated tails for the small wing deflections employed in the present test.

The variation of C_{m_δ} and α/δ with Mach number is shown in figures 11 and 12, respectively. The control effectiveness, as measured by these parameters, although maintained over the Mach number range investigated, was very much lower at the maximum supersonic speeds investigated than at subsonic speeds. However, it should be noted, as shown in figure 10, that the lift produced by unit deflection of the control wing was more nearly constant over the Mach number range. Also shown in figures 11 and 12 are results for a similar configuration from references 3 and 4 transferred to the center of gravity of the present test. The present values are appreciably lower than those from the references and indicate the absence of the effects of downwash at small values of wing incidence previously discussed. This effect is particularly important because, for the present center-of-gravity location, the largest part of C_{m_δ} is due to tail-lift changes caused by wing downwash. Also contributing to the low values of C_{m_δ} were effects of tail elasticity.

Control hinge moments.- The variation of the hinge-moment derivatives, C_{h_α} and C_{h_δ}, with Mach number is shown in figure 13. The results indicate that the control wing was reasonably well-balanced with respect to both deflection and angle of attack over the supersonic Mach number range investigated. At subsonic speeds the control wing was overbalanced. Over the entire Mach number range the center of pressure of the loading due to angle of attack was ahead of that due to wing deflection. Both loadings are indicated to have had a rearward shift near $M = 0.94$, with the angle-of-attack loading having the more abrupt shift. Good agreement is indicated with wind-tunnel tests of a similar configuration at $M = 1.72$ (reference 6). At subsonic Mach numbers fair agreement is obtained between values of C_{h_α} from the present tests and from tunnel tests (reference 3); poorer agreement exists between the flight tests and the tunnel values of C_{h_δ}.

CONCLUDING REMARKS

Preliminary results of a free-flight investigation in the Mach number range from 0.75 to 1.5 of the longitudinal stability and control of a missile model having cruciform, triangular, interdigitated wings and and tails have been presented and are summarized. The center of gravity was located at 50.8 percent of the mean aerodynamic chord of the exposed wing area.

The slopes of the normal-force curves were relatively uniform over the Mach number range and at the maximum supersonic speeds were about 12 percent lower than at subsonic speeds. Static stability existed over the Mach number range investigated and was a maximum at a Mach number of 0.95. Damping was maintained over the Mach number range. The total damping-moment coefficient was considerably lower at supersonic speeds than at subsonic speeds. Control effectiveness, as measured by the increment in trim lift coefficient due to unit wing-deflection angles, was maintained over the Mach number range and was lower at supersonic speeds than at subsonic speeds. The reduction in effectiveness was attributed to the absence of the effects of downwash changes in the vicinity of the tails for the small wing deflections employed. The hinge moments of the control wing were reasonably well-balanced at supersonic speeds and were overbalanced at the lower subsonic speeds.

Langley Aeronautical Laboratory
National Advisory Committee for Aeronautics
Langley Field, Va.

REFERENCES

1. Hall, James R., and Sandahl, Carl A.: Effect of Nose Shape and Wing Thickness Ratio on the Drag at Zero Lift of a Missile Having Triangular Wings and Tails. NACA RM L50C16a, 1950.

2. Gillis, Clarence L., Peck, Robert F., and Vitale, A. James: Preliminary Results from a Free-Flight Investigation at Transonic and Supersonic Speeds of the Longitudinal Stability and Control Characteristics of an Airplane Configuration with a Thin Straight Wing of Aspect Ratio 3. NACA RM L9K25a, 1950.

3. Magnus, R. J., Beal, R. R., and Kutschinski, C. R.: Sparrow 13-D. Analysis of Force and Moment Characteristics from Subsonic Wind-Tunnel Tests of a 50-Percent-Scale Model. Rep. No. SM-13632, Douglas Aircraft Co., Inc., March 15, 1950.

4. Goldbaum, G. C.: Effects of Increased Tail Area, Piping Fairings, and Small Wing Deflections on Force and Moment Data as Measured in the Wind Tunnel on the 13.5-Percent-Scale Model of the Sparrow 13-D at $M = 1.50$. Rep. No. SM-13815, Douglas Aircraft Co., Inc., Sept. 27, 1950.

5. Turner, Robert L., Jr.: Stability and Control Tests of a 0.135 Scale XAAM-N-2 Model in the 19 × 27.5-Inch Mach 1.50 Nozzle. OAL Rep. 112-4, Consolidated Vultee Aircraft Corp., Aug. 29, 1949.

6. Delameter, H. D., Stamper, J. C., and Solvason, J. C.: Model XAAM-N-2 Preliminary Analysis of Force and Moment Characteristics from Supersonic Wind Tunnel Tests of a 45% Scale Semi-Span Model. Mach No. = 1.72. Rep. No. SM-13469, Douglas Aircraft Co., Inc., Aug. 10, 1949.

TABLE I

PHYSICAL CHARACTERISTICS OF MODEL

Weight (loaded), pounds	342
Weight (sustainer motor expended), pounds	301
Moment of inertia in pitch (sustainer motor expended), slug-feet^2	112
Center-of-gravity location (loaded), inches from nose	75.8
Center-of-gravity location (sustainer motor expended), inches from nose	71.3
Center-of-gravity location (loaded), percent mean aerodyanmic chord of exposed wing	75.0
Center-of-gravity location (sustainer motor expended), percent mean aerodynamic chord of exposed wing	50.8
Wing hinge line, percent mean aerodynamic chord of exposed wing	43.0
Exposed area of each wing panel, square feet	1.605
Exposed area of each tail panel, square feet	0.637
Mean aerodynamic chord of exposed wing panel, feet	1.572
Wing section thickness ratio	0.04
Tail section thickness ratio	0.03

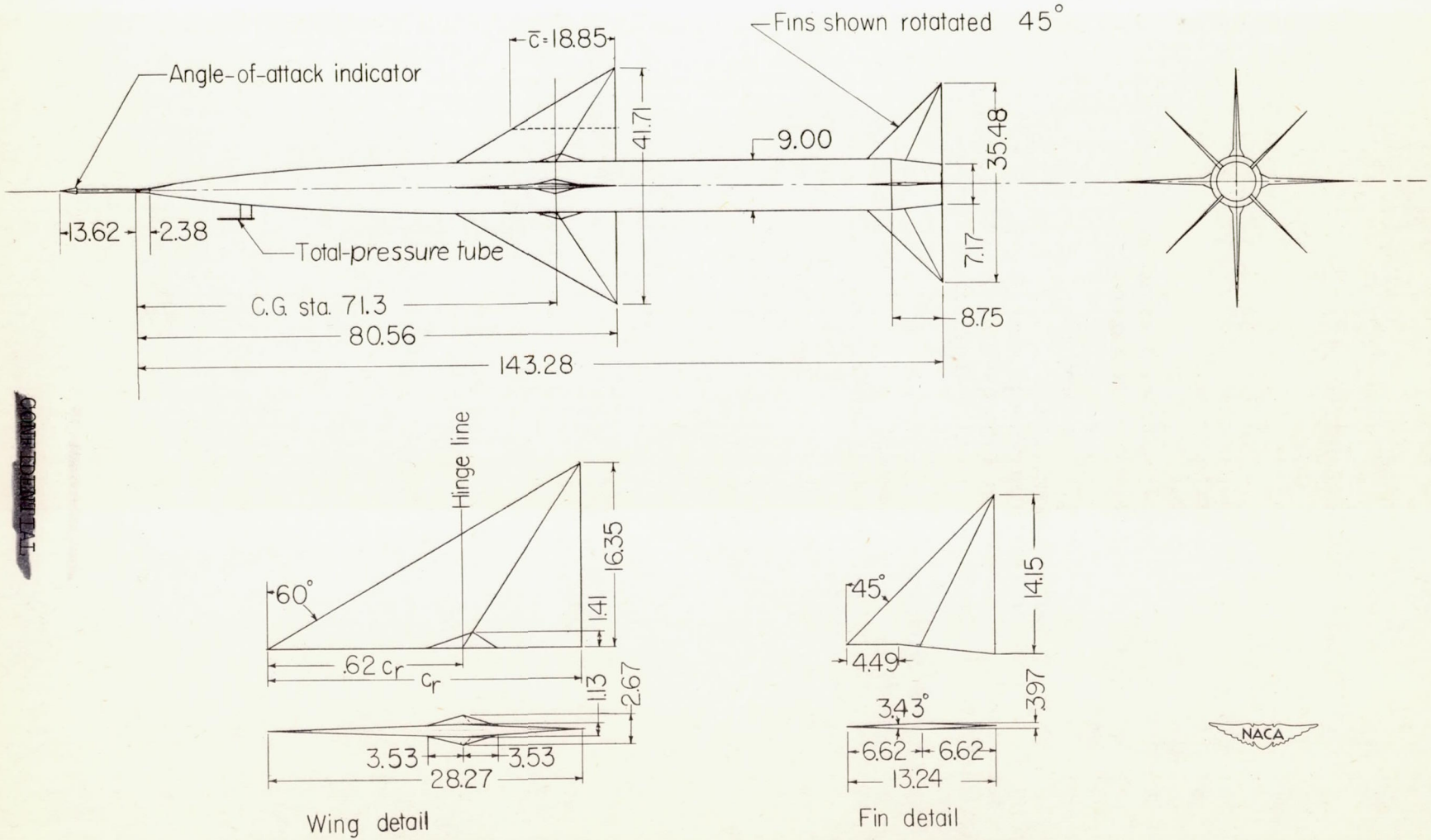

Figure 1.– General arrangement of test vehicle. All dimensions are in inches.

CONFIDENTIAL

CONFIDENTIAL

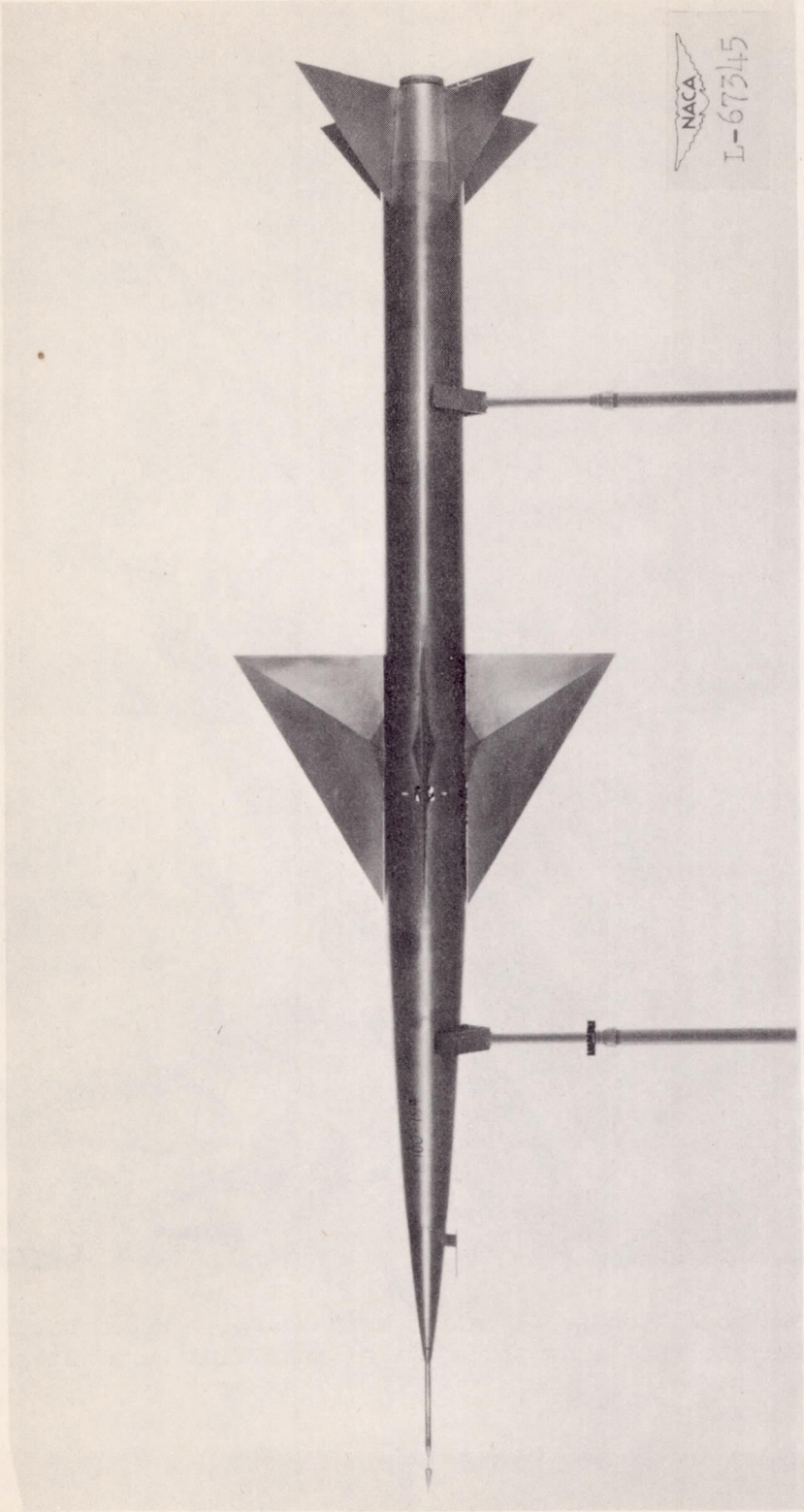

Figure 2.- Subject test vehicle.

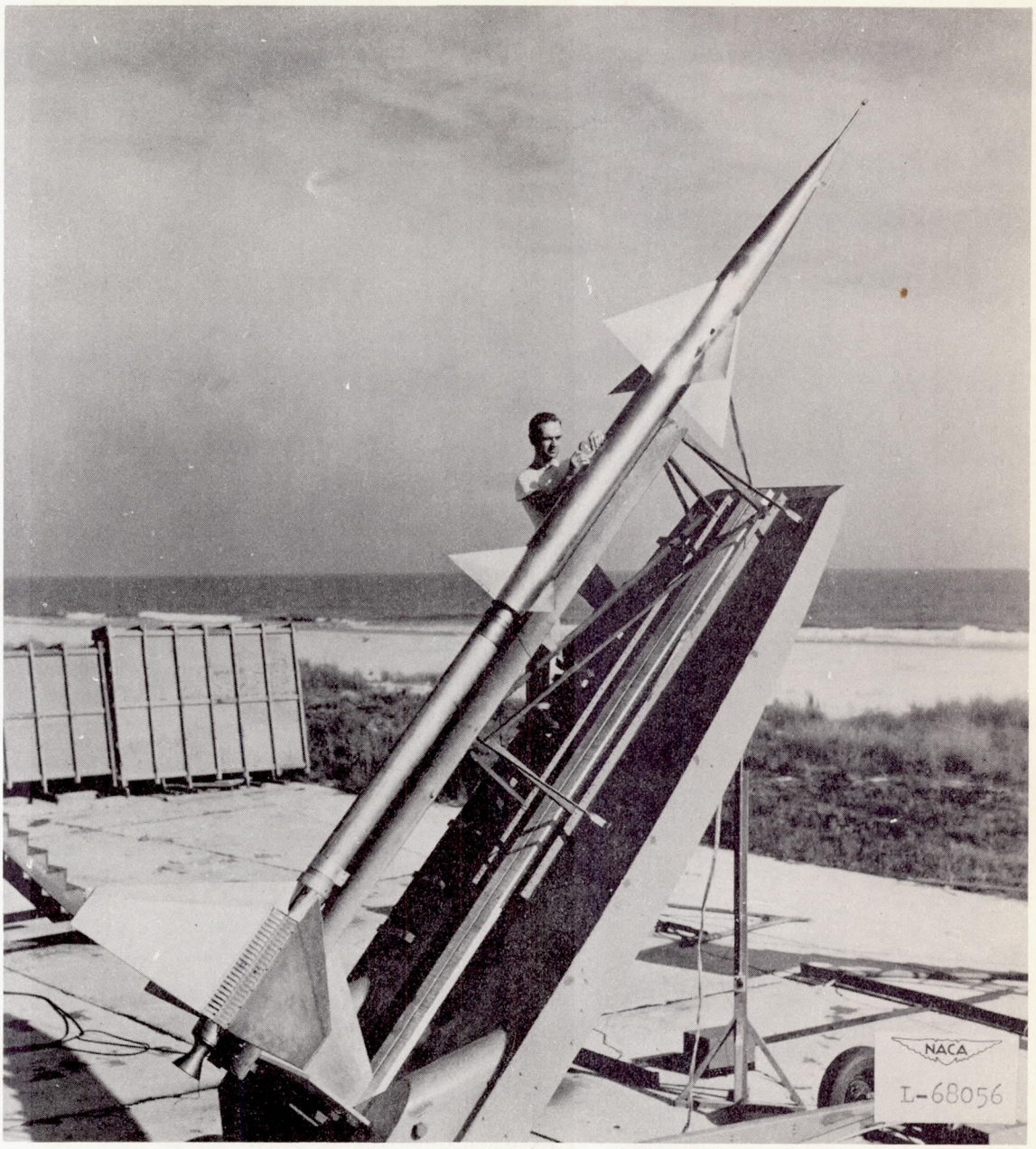

Figure 3.- Typical model-booster-launcher arrangement. Model of present report identical to that shown except that tail fins were interdigitated.

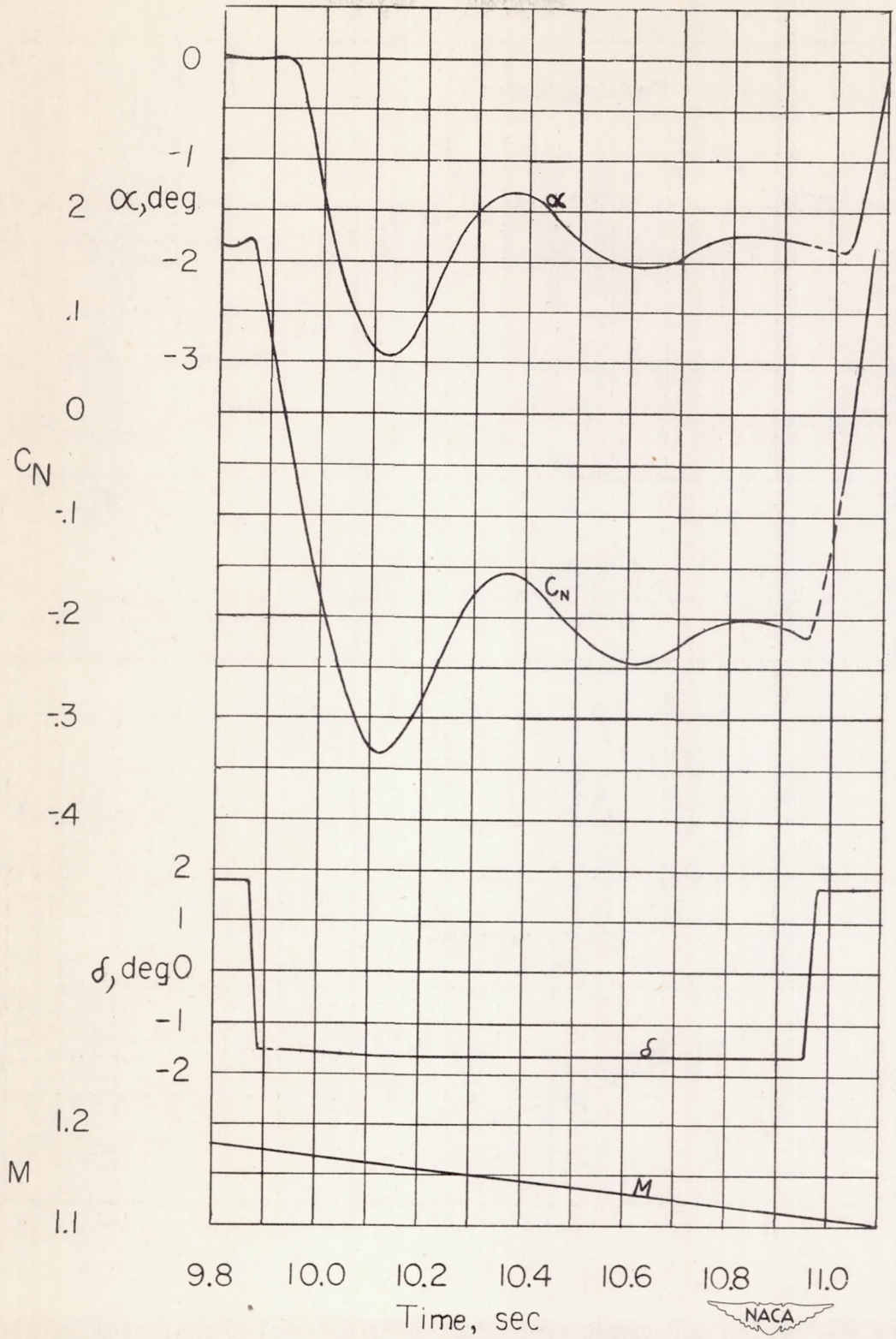

Figure 4.– Typical time history.

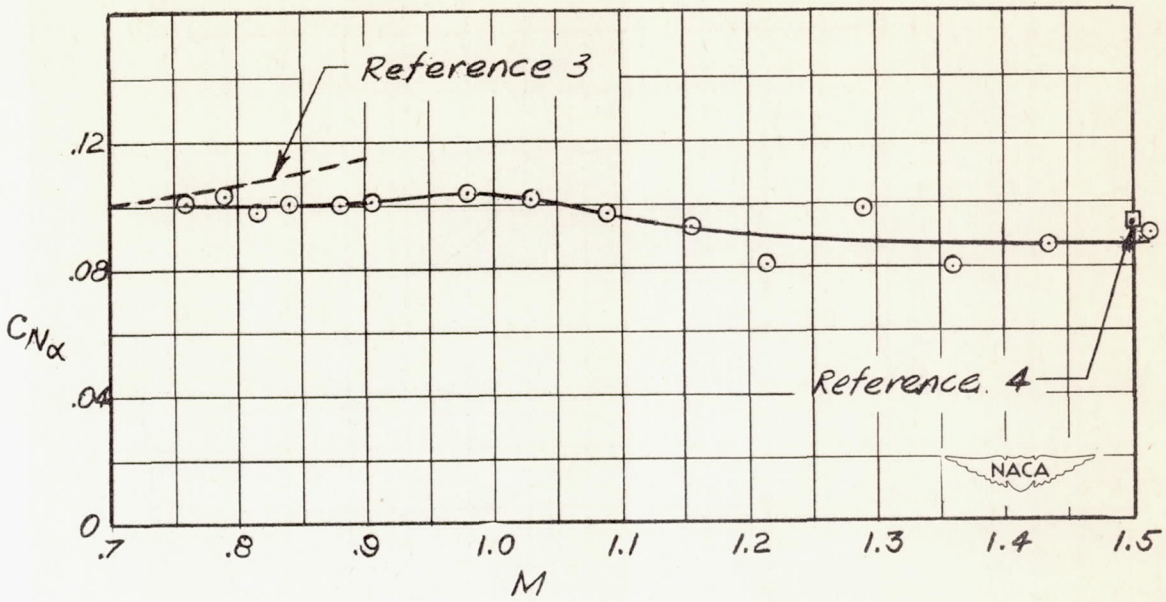

Figure 5.– Variation of normal-force slopes with Mach number.

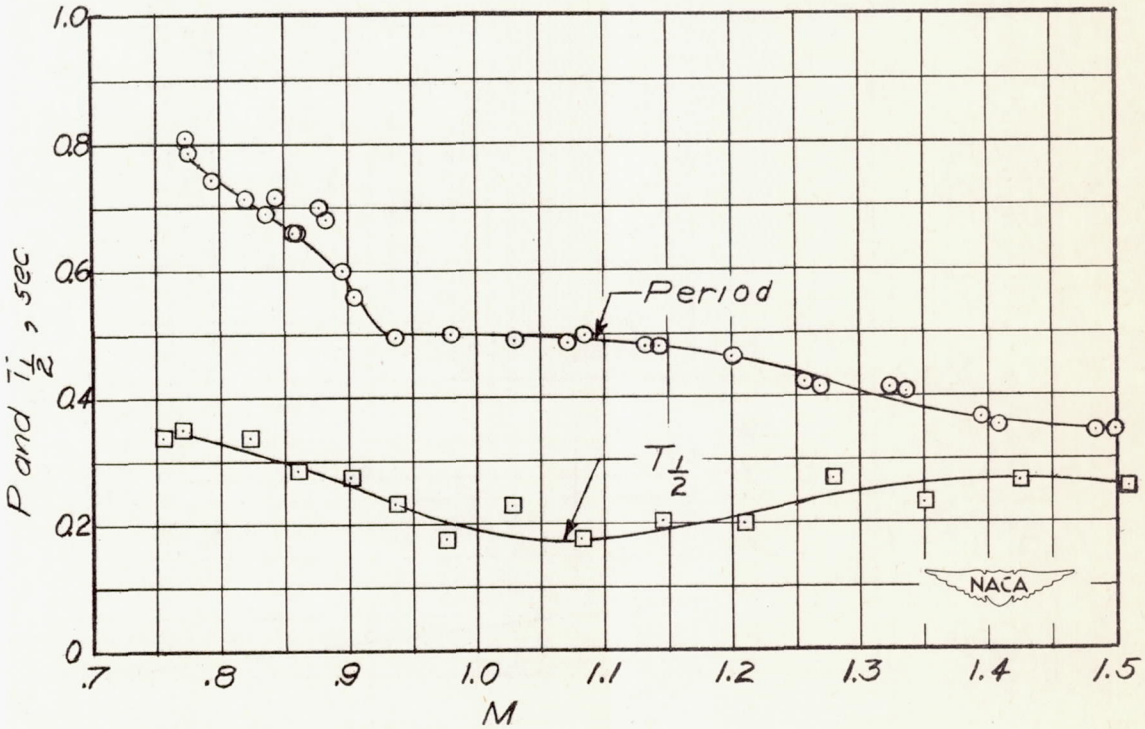

Figure 6.– Period and damping of short-period longitudinal oscillations.

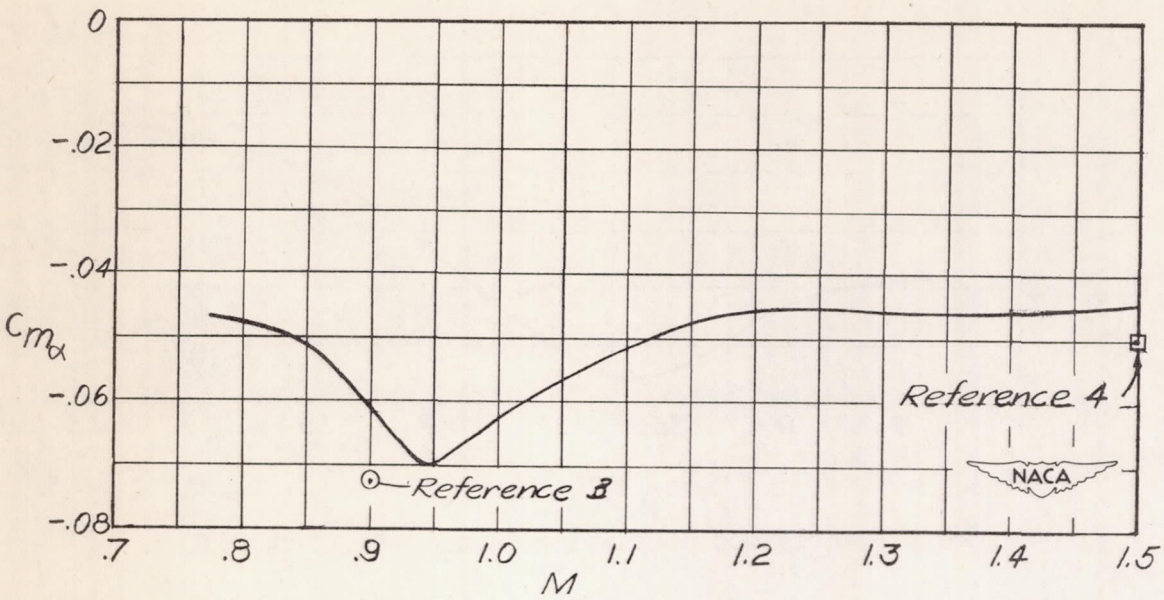

Figure 7.– Variation of static stability with Mach number.

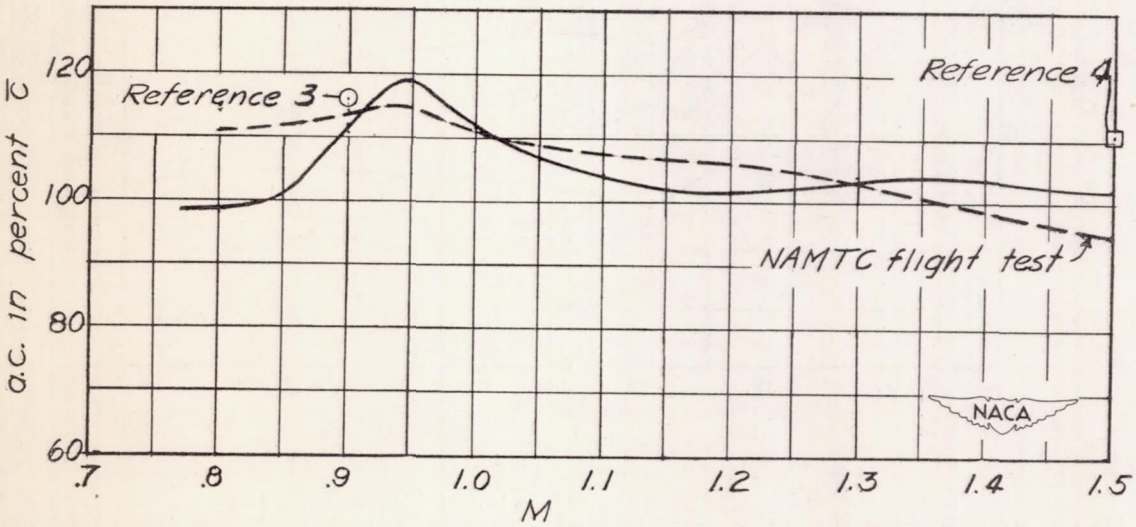

Figure 8.– Variation of aerodynamic center with Mach number.

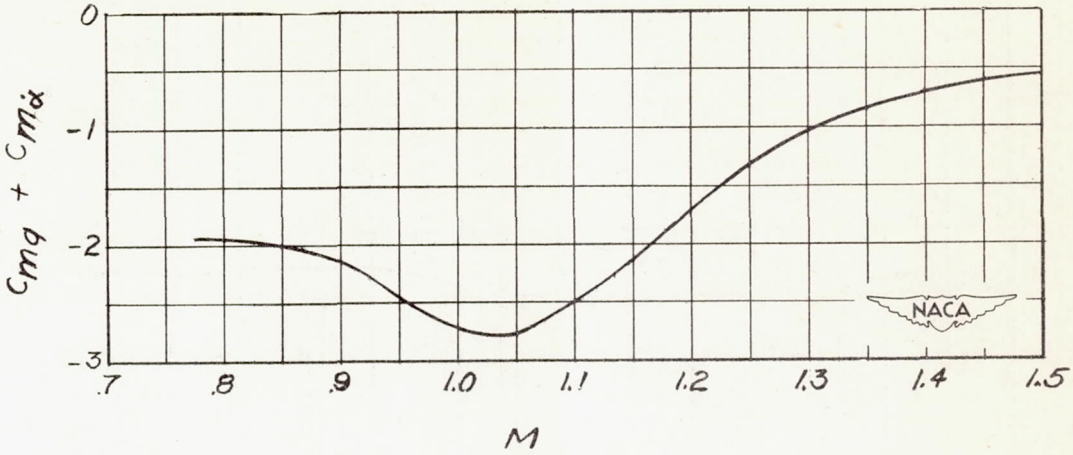

Figure 9.– Variation of damping factor with Mach number.

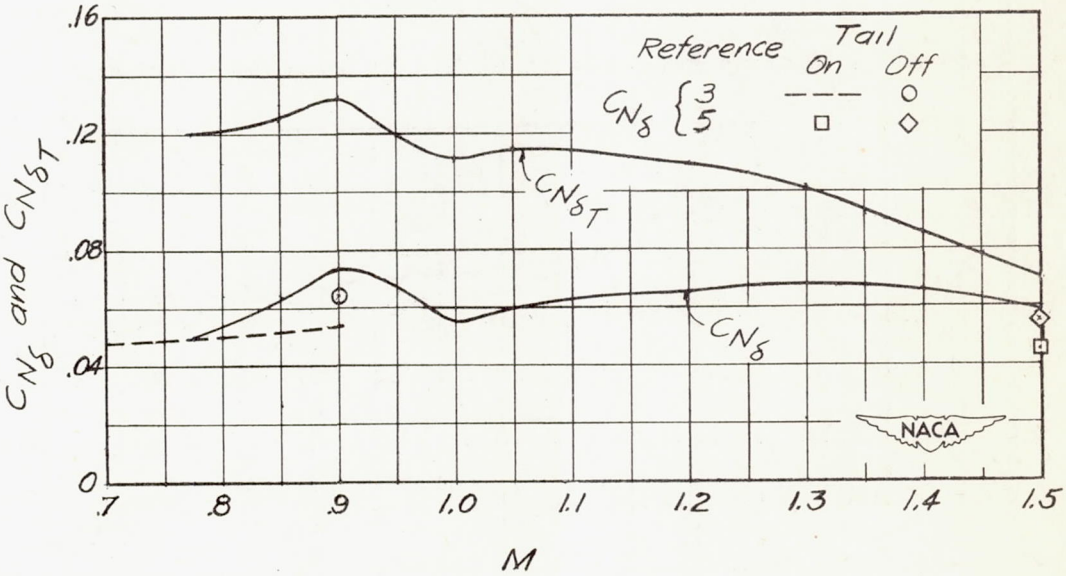

Figure 10.– Variation of normal-force coefficient due to wing deflection angle with Mach number.

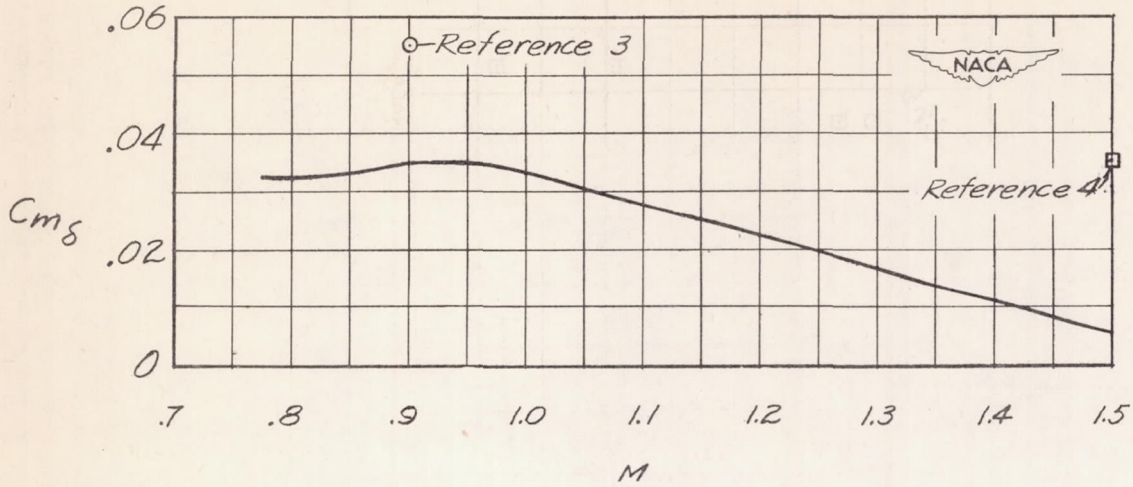

Figure 11.– Variation of pitching-moment coefficient due to wing deflection angle with Mach number.

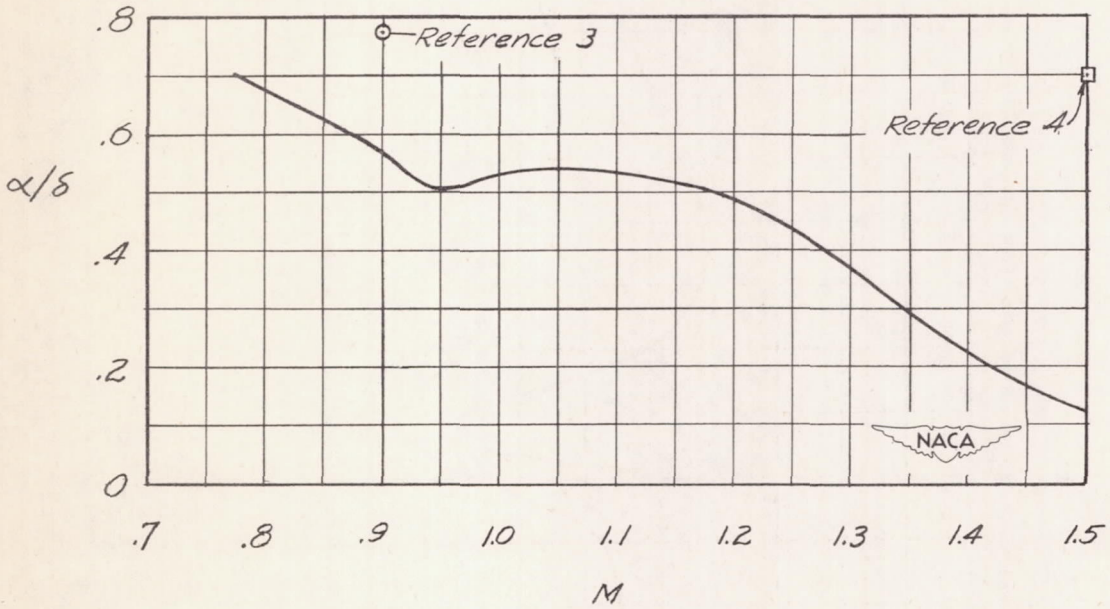

Figure 12.– Variation of angle-of-attack change due to unit wing deflection angle with Mach number.

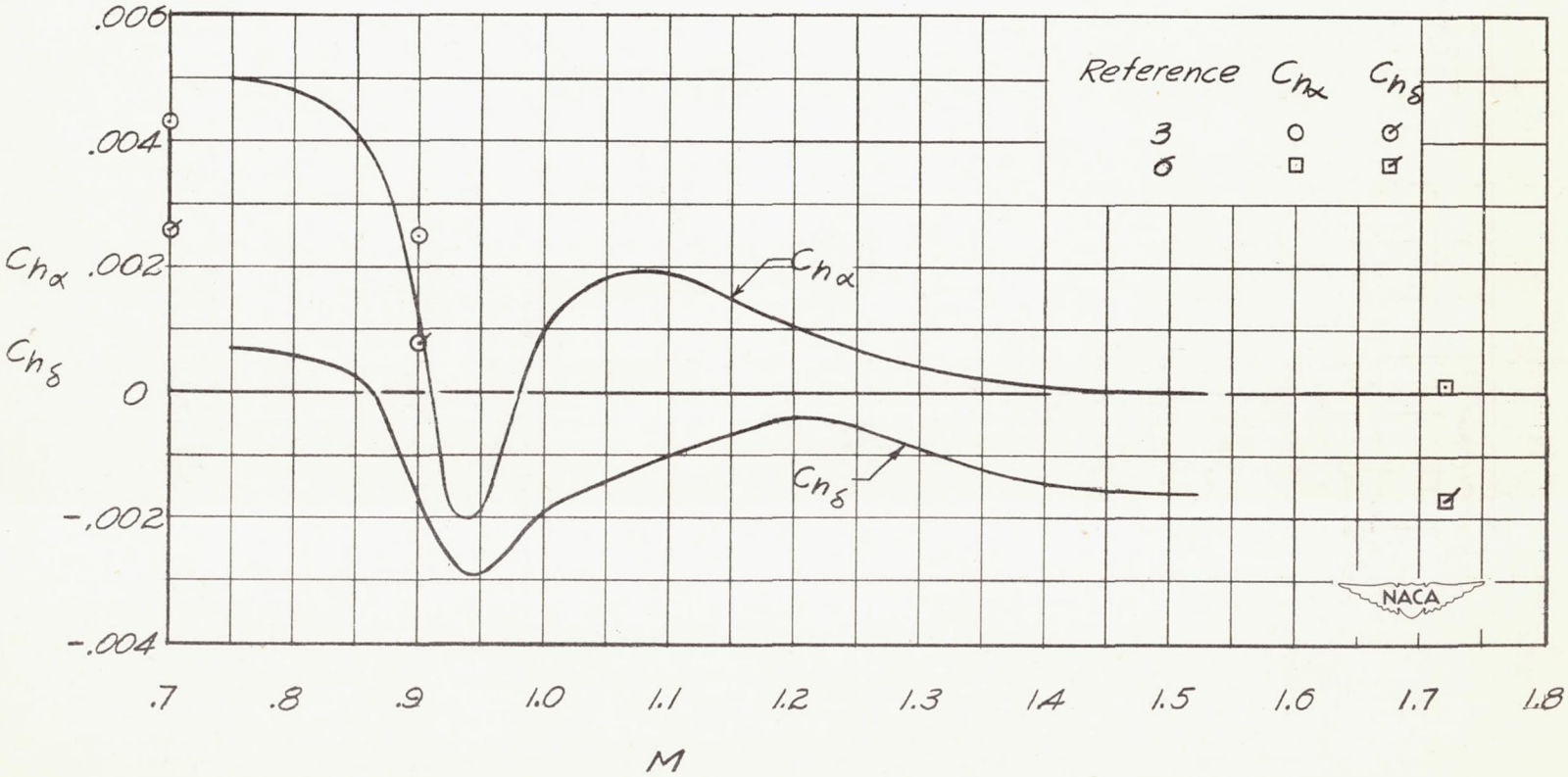

Figure 13.- Variation of hinge-moment derivatives with Mach number.

[redacted]

NACA-Langley - 7-10-51 - 400

DECLASSIFIED

CONFIDENTIAL

DECLASSIFIED

CONFIDENTIAL